Thermochimica Acta, 128 (1988) 267–295
Elsevier Science Publishers B.V., Amsterdam – Printed in The Netherlands

BIOLOGICAL THERMODYNAMIC DATA FOR THE CALIBRATION OF DIFFERENTIAL SCANNING CALORIMETERS: HEAT CAPACITY DATA ON THE UNFOLDING TRANSITION OF RIBONUCLEASE A IN SOLUTION

FREDERICK P. SCHWARZ and WILLIAM H. KIRCHHOFF

Chemical Thermodynamics Division, National Bureau of Standards, Gaithersburg, MD 20899 (U.S.A.)

(Received 15 September 1987)

ABSTRACT

Extensive measurements of the heat-capacity changes accompanying the unfolding transition of bovine pancreatic ribonuclease A in buffered aqueous solutions have been performed in a differential scanning calorimeter over a range of experimental conditions. The concentration of ribonuclease A varied from about 1 to 2 mass%. The pH varied from 1.8 to 5.0 at two glycine–HCl buffer concentrations: 0.1 and 0.2 M. Measurements were made on ribonuclease A obtained from various commercial sources. The heat capacity data were corrected for the thermal lag of the instrument and fitted by least-squares to a two-state model to determine the transition enthalpy and temperature, the heat-capacity change in the baseline, and the cooperativity of the transition. The transition temperature T_m and enthalpy ΔH_m determined from the fit of a two-state model to the transition profile increased linearly with pH from 311.9 ± 0.5 K and 308.2 ± 6.4 kJ mol^{-1} at pH = 2 to 335.4 ± 0.6 K and 408.9 ± 6.6 kJ mol^{-1} at pH = 4, where the uncertainties represent two standard deviations based on a linear least-squares fit of ΔH_m and T_m to pH. Values of T_m and ΔH_m were independent of the commercial source of ribonuclease A. The value of T_m was independent of the buffer concentration but showed a slight dependence on the concentration of ribonuclease A. On the other hand, ΔH_m was independent of concentration of ribonuclease A, but showed a slight dependence on the concentration of the glycine buffer solution. The heat capacity change obtained from the change in the transition baseline at T_m was 3.4 ± 0.5 kJ mol^{-1} K^{-1} averaged over all determinations. The cooperativity of the transition, that is the ratio of the number of moles participating in the transition as determined from the two-state model to the actual number of moles in the sample, varied from 0.91 ± 0.02 at pH 2 to 1.07 ± 0.02 at pH 4 compared with unity for an ideal, two-state transition with a stoichiometry of one.

INTRODUCTION

Differential scanning calorimetry provides information on the enthalpy, temperature, and heat capacity changes that accompany conformational transitions of biological molecules in solution. Differential scanning calorimeters (DSCs) specifically designed for such studies typically employ sample

0040-6031/88/$03.50

volumes of about 1 ml and operate over a temperature range from below 253 to about 400 K. Measurement precision is typically on the order of 0.5 μW, 0.1 K, and 0.1 mJ K^{-1}. In spite of the prevalent use of such DSCs, accurate thermal data for well-characterized biological materials are not readily available for verification of instrument calibration and performance. In order to achieve high precision measurements, many DSCs contain fixed sample cells which are filled through capillary tubes. Such cells cannot be calibrated with currently available temperature and enthalpy standards which undergo solid to liquid phase transitions in this temperature range.

An important feature in the analysis of DSC measurements is the shape of the excess heat-capacity transition profile which depends both on the detailed molecular pathways and dynamics leading to the conformational change and on the instrumental response time. One would like to extract as much information as possible on the molecular dynamics accompanying the conformational changes. The instrumental response time can be accounted for only approximately through the analysis of pulse heating measurements. Reference data from well-characterized materials with well-characterized profile shapes can be useful in distinguishing instrumental from sample effects.

From the perspective of sample size, operating conditions, attainable measurement precision, compatibility with fixed sample cells, and analysis of the excess heat-capacity transition profile shape, colloidal suspensions of lipids or solutions of proteins exhibiting well-characterized phase transitions in suitable temperature ranges provide the most useful sources of thermal data for DSC evaluation and/or calibration. A recent study [1] of the phase transitions exhibited by suspensions of di-alkylphosphatidylcholines in buffered aqueous solutions has shown that the transition enthalpies of these lipids depend in an unpredictable way on sample preparation and storage conditions, thereby limiting their usefulness as a source of reproducible data for the evaluation of instrument performance. In the present study, the conformational transitions exhibited by ribonuclease A in solution are studied for their suitability as a source of accurate, reproducible thermal data for evaluating DSC performance.

The unfolding transition of bovine pancreatic ribonuclease A, a globular polypeptide consisting of 124 amino acid residues, in buffered aqueous solutions has been studied extensively over the past two decades by differential scanning calorimetry [2–7]. Ribonuclease A catalyzes the breakdown of ribonucleic acid in two steps: breakage of the phosphodiester linkage to a 2′,3′-cyclic phosphate followed by hydrolysis of the cyclic phosphate nucleotides to yield a terminal pyrimidine 3′-phosphate [8]. From measurements on dilute solutions (0.05–0.5 mass%), Privalov and Khechinashvili [6] have shown that the enzyme undergoes a transition from a natural folded configuration to a so-called random coil when heated from room temperature to 353.14 K and that the transition temperature and enthalpy depend

upon the pH of the solution. More specifically, the transition temperature and enthalpy increase from 307.14 K and 382.8 kJ mol^{-1} at pH 2.75 to 337.1 K and 481.2 kJ mol^{-1} at pH 5.74 [6]. In a later study, Sochava et al. [7] observed a similar dependence of the transition temperature and enthalpy on the pH of the ribonuclease A buffered solution at a higher concentration of 15 mass%.

Critically important requirements for a material whose thermodynamic properties are to provide reproducible thermal data are the stability of the material and the ease and reliability with which its concentration can be determined. Ribonuclease A is fairly stable and solutions of ribonuclease A can be analyzed by simple kinetic techniques [9,10] based on its catalytic properties and UV absorption spectrum.

In this study, the excess heat capacity of ribonuclease A in various buffered aqueous solutions has been measured as a function of temperature. The transition temperature, transition enthalpy, and heat capacity change accompanying the transition have been determined by fitting the excess heat capacity data with a model that describes the unfolding transition in terms of a two-state transition [11,12]. In this model, the shape of the transition profile is analyzed in terms of a molar enthalpy change accompanying the transition from the low temperature folded state to the high temperature unfolded state, the number of moles of material undergoing the transition, and a baseline whose shape is determined by the mole fractions of the low- and high-temperature species coexisting at intermediate temperatures throughout the transition interval. The mole fractions of low- and high-temperature species are determined by the extent of reaction as evidenced by the shape of the excess heat-capacity transition profile above the baseline.

The shape of the transition profile is a function of the stoichiometry of the transition. Profiles of transitions of the type $A \rightarrow nB$ and $nA \rightarrow B$ will differ and will depend upon the value of n. For example, Takahashi and Sturtevant were able to deduce the stoichiometry of the denaturation of the protein *Streptomyces* subtilisin inhibitor by comparing the closeness of fit of the two-state model as a function of n [12]. For an assumed stoichiometry, the two-state analysis provides a value for the number of moles of material undergoing the transition in addition to the transition temperature, transition enthalpy and heat capacity change in the baseline. The comparison between the number of moles of participating material determined from the two-state analysis with the number of moles in the DSC cell as determined by an independent method of analysis allows one to determine the cooperativity of the transition and thus confirm its stoichiometry. For the ribonuclease A transition, the value of n is close to 1.

In this study, we have compared the values of the transition enthalpy obtained from the two-state analysis with the values obtained from a linear baseline interpolation under the transition profile and with the results of a van't Hoff analysis (log K vs. $1/T$, where K is the equilibrium constant, T

is the temperature, and d(log K)/d($1/T$) is assumed to be constant) of the transition profile. Effects of variation in the source, purity, and concentration of the ribonuclease A, pH, and buffer concentration on the transition enthalpy and temperature and excess heat-capacity change in the baseline have been determined in order to evaluate the sensitivity of the thermodynamic data to experimental conditions.

EXPERIMENTAL

Materials

Four samples of bovine pancreas ribonuclease A were obtained from three different commercial sources and are identified with the lables *a–d*. Sample *a* from source number 2 had a stated purity of 90%. Sample *b*, also from source number 2, had a stated purity of 70% and had been stored in a freezer for seven years. Sample *c* was from source number 3 and had a stated purity of 87%. Sample *d* was from source number 1 and had a stated purity of 98%. A sodium dodecylsulfate gel electrophoresis analysis [13] was performed on all the samples to determine their actual purity. The sulfuric acid, glycine, hydrochloric acid, sodium chloride, sodium hydroxide, sodium acetate, acetic acid, and tris-(hydroxymethyl)-aminomethane (Tris) were reagent quality. The bakers yeast ribonucleic acid was type 3 from Sigma Chemical Co. and was used without further purification *. The sodium cytidine 2′,3′-cyclic monophosphate was 98% pure.

Preparation and analysis of solutions

Solutions having a concentration of 2 mass% were prepared by dissolving ribonuclease A in a 0.2 M glycine–HCl solution buffered at pH 4.0. The glycine buffer was prepared by dissolving 0.2 M of glycine in 1 liter of distilled water and adding conc. HCl dropwise until the pH reached 4.0 as monitored by an Orion 811 pH meter operated with a Corning EX-L glass electrode. A few solutions were prepared at a lower concentration of ribonuclease A and also in a 0.1 M glycine–HCl buffered solution to determine the effect of ribonuclease A or buffer concentration on the thermodynamic data. About 10 ml of solution were prepared and dialyzed

* Certain commercial equipment, instruments and materials are identified in this paper in order to specify the experimental procedure as completely as possible. In no case does such identification imply a recommendation or endorsement by the National Bureau of Standards, nor does it imply that the material, instrument, or equipment identified is necssarily the best available for the purpose.

using a membrane with a molecular weight cut-off of 3500 against a volume of about 400 ml of the buffer solution to remove low-molecular-weight impurities. During the course of the dialysis, which lasted about twenty-four hours, the buffer solution was changed three times. If the solution was not dialyzed, impurities which absorbed ultraviolet light below 300 nm interfered with the spectrophotometric analysis of ribonuclease A at 278 nm. Ribonuclease A solutions were stored in the dark in a refrigerator at 277 K when not being used to prepare samples for the DSC measurements and were found to be stable for periods up to a month as judged by spectrophotometric analysis, enzymatic activity, and consistency with experimental calorimetric data. Prior to the DSC measurement, a 2-ml aliquot of solution was adjusted to the desired pH by the addition of HCl or NaOH and a portion was set aside for analysis by UV spectroscopy. For the spectroscopic analysis, the ribonuclease A solution was diluted to a concentration of about 0.1 mass% with a measured mass of 0.2 M Na_2HPO_4–NaH_2PO_4 buffer at pH 7.0. The optical density was measured at 278 nm with a Perkin Elmer Lambda 4B spectrophotometer, and the concentration determined using a value of the optical density of a 0.1 mass% ribonuclease A solution of 0.738 at 278 nm [6].

In order to validate the results of the spectroscopic analysis, aliquots of the dialyzed 2 mass% solutions prepared from each of the four different sources of ribonuclease A were analyzed by two enzymatic assays. Aliquots were diluted to the microgram per liter range for the assays. In the Kunitz enzymatic assay procedure [9], 2 ml of the diluted ribonuclease A solution were mixed with an equal volume of a solution of 0.1 mass% bakers yeast ribonucleic acid in 0.1 M sodium acetate buffer (pH 5.0). The decrease of the UV absorption of ribonucleic acid resulting from breakage of its diphosphoester bonds was monitored at 300 nm as a function of time. The enzymatic activity as defined in terms of Kunitz units is the number of micrograms of enzyme in a 1-ml sample of the ribonuclease A solution required to decrease the optical density by 1.0 at 300 nm in 1 min under the conditions of the assay. In the enzymatic assay procedure of Crook et al. [10], a solution of 0.1 g l^{-1} sodium cytidine 2′,3′-cyclic monophosphate in 0.1 M Tris buffer (pH 7.0) was substituted for the ribonucleic acid solution and the increase in the hydrolysis of the cyclic phosphate ring was monitored at 284 nm as a function of time. The initial reaction rate in units of the increase in absorbance per minute was compared with literature values for the rate to obtain the concentration of enzyme present in the solution.

DSC measurements

DSC measurements were performed with a Hart 7707 DSC heat conduction scanning microcalorimeter consisting of two matched pairs of removable cylindrical cells. Two samples were scanned simultaneously with each

sample cell run against a reference cell containing an equal mass of the buffer solution. The calibration and the operating characteristics of the DSC have been described previously [1]. Temperature calibrations were performed at 10 K intervals with a Type E thermocouple which had been calibrated by the NBS Temperature and Pressure Division. Previous determinations of the transition temperatures and enthalpies of the thermal denaturation of defatted human serum albumin-octanoate solutions using the Hart DSC differed by less than 0.1 K and 3% respectively from the transition temperatures and enthalpies measured by Ross (unpublished results) with a DSC designed by Ross and Goldberg, using narrow rectangular cells [14]. The Hart DSC was operated at a scan rate of 18 K h^{-1} and the solution mass in the cells varied from 0.5 to 0.85 g. The relation of the calorimeter sensor output to the instantaneous calorimeter power input over the temperature range of the experiments was measured with built-in calibration heaters as described previously [1]. The power input from a thermal scan of buffer versus buffer over the same temperature range and at the same scan rate was subtracted from the power input of each ribonuclease A solution versus buffer scan to minimize, as much as possible, systematic differences between the cells.

Data analysis

All the net power transition profiles were corrected for the effect of time lag thermal gradients in the instrument by application of the Tian equation [15]

$$W = W_0 + \tau(dW_0/dt) \tag{1}$$

where W is the corrected power, W_0 is the observed power, τ is the exponential response time of the instrument, and dW_0/dt is the rate of change of differential power values with time t. The response time of the DSC (138 s) was determined from a least-squares fit of the shape of a calibration heater pulse, with the cells filled with buffer solution, to an exponential decay function. To determine the value of dW_0/dt at each data point, W_{0i}, a linear fit of W_0 to five data points symmetrically placed about W_{0i} was performed and the slope of the fit was used as the value of dW_0/dt at W_{0i}. This method of calculating dW_{0i}/dt was used to reduce random error in the evaluation of dW_0/dt without introducing signal distortion arising from non-linearities in the profile shape. Even for the slow scan rates of 18°C h^{-1} used in this study, the data must be corrected for the time response of the instrument. Transformation of the primary calorimetric data using the Tian equation led to a correction factor of -0.7 K in the reported transition temperatures, but little change in the enthalpy values.

The corrected net power versus temperature profiles were then converted to net heat capacity (hereafter termed excess heat capacity) versus tempera-

ture profiles by dividing the net power at each temperature by the scan rate. To evaluate the scan rate, the temperature over the thermal scan was fit to a cubic power series in time. The scan rate, dT/dt, as a function of time was then evaluated for each datum from the analytic derivative of the cubic function.

To determine the transition temperature, transition enthalpy, and the change in the excess heat capacity of the baseline, the excess heat capacity versus temperature profiles were fit to a model [11,12] which describes the phase transition in terms of two states (species) in equilibrium. If $\Delta H = H_B - H_A$ is the enthalpy change at a temperature T resulting from conversion of one mole of A to B, then the heat dQ needed to raise the temperature of the protein solution relative to the reference solution by an amount dT is given by

$$dQ = \Delta H\, dN_B + \left(N_A C_{pA} + N_B C_{pB}\right) dT \tag{2}$$

where N_A is the number of moles of A, N_B is the number of moles of B, and C_{pA} and C_{pB} are the molar heat capacities of species A and B respectively. N_A and N_B can be evaluated from the equilibrium constant K for unit stoichiometry

$$K = N_B/N_A \tag{3}$$

and from the total number of moles of material N

$$N = N_A + N_B \tag{4}$$

The temperature dependence of N_A and N_B is obtained from the temperature dependence of the equilibrium coefficient

$$K = e^{-\Delta G/RT} \tag{5}$$

From eqns. (3) and (4)

$$N_B = \frac{NK}{1+K} \tag{6}$$

and

$$dN_B/dT = \frac{N}{(1+K)^2} dK/dT = -\frac{NK}{R(1+K)^2} \frac{d(\Delta G/T)}{dT} \tag{7}$$

From the Gibbs–Helmholz equation

$$\left(\frac{\partial(\Delta G/T)}{\partial T}\right)_p = -\Delta H/T^2 \tag{8}$$

we obtain, on substitution of eqns. (6)–(8) in eqn. (2)

$$dQ/dT = \frac{N\Delta H^2/RT^2}{(1+K)(1+1/K)} + NC_{pA} + \frac{N\Delta C_p}{(1+1/K)} \tag{9}$$

The temperature dependence of ΔH can be expressed as a power series in T about T_m, the midpoint of the transition where the area under the transition profile is half the total area

$$\Delta H = \Delta H_m + \Delta C_p(T - T_m) \tag{10}$$

The temperature dependence of K can be obtained by substituting eqn. (10) into the Gibbs–Helmholz equation and integrating between T and T_m to give

$$\Delta G/RT = \frac{\Delta H_m(T - T_m)}{RTT_m} + \frac{\Delta C_p}{R} \ln(T/T_m) + \frac{\Delta C_p(T - T_m)}{RT} \tag{11}$$

where the standard state temperature T_m is the temperature at which $K = 1$ and the number of moles of species A and B are equal. ΔG is then the free energy change required to bring the system to this standard state.

Finally, it is assumed that C_{pA} and ΔC_p, where they appear explicitly in eqn. (9), vary linearly with temperature

$$C_{pA} = C_{pA} + C'_{pA}(T - T_m) \tag{12a}$$

and

$$\Delta C_p = \Delta C_p + \Delta C'_p(T - T_m) \tag{12b}$$

Equations (9)–(12) can be combined and the parameters ΔH_m, T_m, N, C_{pA}, C'_{pA}, ΔC_p and $\Delta C'_p$ evaluated for each thermal scan from least-squares fits of the excess heat capacity–temperature data sets.

Several points are worth noting. The number of moles N of material undergoing the transition appears as a variable parameter and is obtained directly from the least-squares analysis. The value of ΔH_m is the molar enthalpy. The integral of eqns. (9)–(12) above the baseline, that is the integral of the first term in eqn. (9), is $N\Delta H_m$ and is generally referred to as the calorimetric enthalpy. The baseline itself has a sigmoidal shape arising from the temperature dependence of K in the third term of eqn. (9). This sigmoidal baseline represents the average heat capacity of species A and B weighted by their mole fractions as a function of temperature.

In general, the two-state model is only approximate. Concerted configurational changes within the protein can occur which are independent of the main conformational transition. Moreover, the denaturation does not necessarily erase all vestiges of the original secondary structure. Experimental artifacts such as incomplete cancellation of differences between the sample and reference cells can lead to temperature-dependent trends in the baseline. In fact, fitting the two-state model to the thermal scan data of ribonuclease A results in residuals $(dQ/dT)_{obs} - (dQ/dT)_{calc}$ exhibiting a systematic dependence on T that is an order of magnitude greater than the random scatter in the data. As a result, a statistical analysis of variance is not meaningful and the standard errors of the parameters contained in the

variance–covariance matrix of the least-squares fit cannot be used to estimate confidence intervals for the parameters. Moreover, systematic trends in the baseline make the interpretability of the baseline in terms of the heat capacities of the two states somewhat dubious, with the exception that the difference between the asymptotic linear baselines, extrapolated to T_m, gives a reasonable estimate of $N\Delta C_p$.

Accordingly, the following procedure has been used for calculating the thermodynamic parameters and the number of moles of material undergoing the transition. The high- and low-temperature asymptotic baselines are determined independently from data sufficiently above and below the transition temperature region to eliminate any contribution from the transition data. This elimination of transition contributions can be tested by varying the data included in the evaluation of the pre- and post-transition baselines. The determination of the asymptotic baselines provides the values of C_{pA}, C'_{pA}, ΔC_p and $\Delta C'_p$ to be used in eqns. (9) and (12). The excess heat capacity data in the transition region are then used to calculate N, ΔH, and T_m from eqns. (9)–(12) while holding the values of C_{pA}, C'_{pA}, ΔC_p and $\Delta C'_p$ fixed. When this procedure is compared with the procedure of minimizing the variance by varying all parameters simultaneously, the least-squares fit is seen to deteriorate as judged by the increase in the standard deviation of the fit (as expected) but to improve, in the case of ribonuclease A, as judged by the agreement of N with the value of N determined by the spectroscopic and enzymatic analyses. The reason for this lies in the fact that deviations from the two-state model are likely to occur in the wings of the transition. The baselines, when they are simultaneously varied with the transition parameters, are thus shifted to accommodate the deviations from the two-state model. Shifts in the baseline have a pronounced affect on the value of N.

The procedure of determining separately the upper and lower asymptotic baselines is one that gives an improved value for N and one for which systematic deviations due to departures from the two-state model are more easily visualized when the residuals are examined. However, in order to estimate the uncertainty in the determined values of N, ΔH, T_m, and ΔC_p, the scan to scan variability in these parameters (discussed below) must be relied upon, and not the statistics of the least-squares fit itself.

RESULTS AND DISCUSSION

Purity and activity analysis

The results of the SDS electrophoresis and enzymatic activity analyses of the ribonuclease A solutions are summarized in Table 1. SDS electrophoresis analysis of the ribonuclease A samples revealed the presence of only one band at 14 kDal for samples *b* (70% purity) and *d* (98% purity) whereas

TABLE 1

Comparison of analyses of dialyzed ribonuclease A solutions

Sample	Ratio of enzymatic analysis to spectroscopic analysis [a]		SDS gel electrolysis
	Kunitz / Spectroscopic	Crook / Spectroscopic	
a 90% pure (1985) from source 1	0.77 ± 0.12	0.97 ± 0.09	Two bands, one at 14 kDal and a weak one at 18 kDal
b 70% pure (1979) from source 1	0.90 ± 0.06	0.96 ± 0.11	One band at 14 kDal
c 87% pure (1985) from source 2	0.81 ± 0.03	1.02 ± 0.09	Two bands, one at 14 kDal and a faint one at 18 kDal
d 98% pure (1985) from source 3	0.95 ± 0.06	0.95 ± 0.06	One band at 14 kDal

[a] Spectroscopic analyses were made at a wavelength of 278 nm.

both *a* (90% purity) and *c* (87% purity) exhibited an intense band at 14 kDal and a weaker band at 18 kDal. The band at 14 kDal corresponds to pure ribonuclease A which has a molecular weight of 13.7 kDal.

All concentrations determined by the procedure of Crook et al. [10] were within experimental error of the concentrations determined by the spectroscopic analysis. Similarily, with the exception of the sample *c*, all concentrations determined by the Kunitz analysis [9] were within experimental error of the concentrations determined by the spectroscopic analysis. Apparently, the presence of the 18 kDal impurity in samples *a* and *c* had no consistent effect on the comparison of the enzymatic assays with the spectroscopic analysis. Either the impurity does not absorb at 278 nm or, more likely, the impurity is too low in concentration to be detected at 278 nm. Independently of variation in the commercial source and purity of the ribonuclease A, all the dialyzed solutions of ribonuclease A exhibit the same amount of enzymatic activity per gram of material, and thus the same amount of native ribonuclease A.

DSC Measurements

Typical thermal scans of 2 mass% ribonuclease A in 0.2 M glycine buffer solutions in the pH range 2.0–4.0 are shown in Figs. 1–3 along with the computer simulated excess heat capacity curves from the two-state model. Both the pre-transitional and post-transitional baselines increase linearly

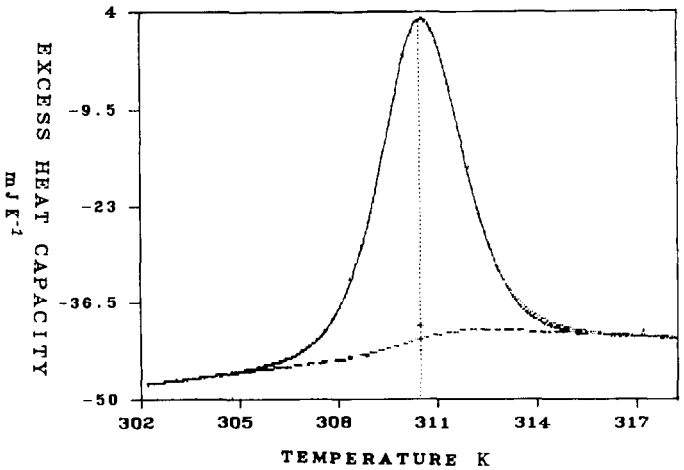

Fig. 1. DSC thermal scan number 9 (1.85 mass% ribonuclease A in 0.2 M glycine buffer at 2.24 pH) scan rate = 18 K h^{-1}. Two-state model curve (· · · · · ·). Only the two-state model baseline under the transition curve is distinguishable.

with temperature as observed by others [6]. All measured transitions appear to be single-peak, symmetrical transitions, the peaks become narrower with increase in the transition temperature. An increase in the excess heat capacity of the solution as ribonuclease A unfolds from its natural state to its denatured state was also observed as a positive difference in the baselines extrapolated to T_m.

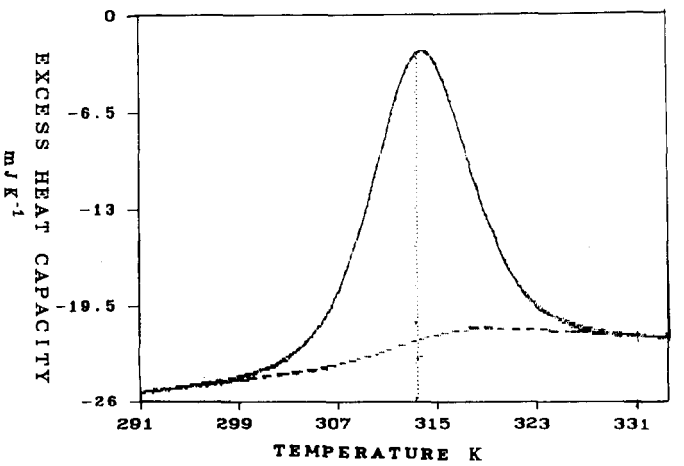

Fig. 2. DSC thermal scan number 39 (2.07 mass% ribonuclease A in 0.2 M glycine buffer at 3.15 pH) scan rate = 18 K h^{-1}. Two-state model curve (· · · · · ·). Only the two-state model baseline under the transition curve is distinguishable.

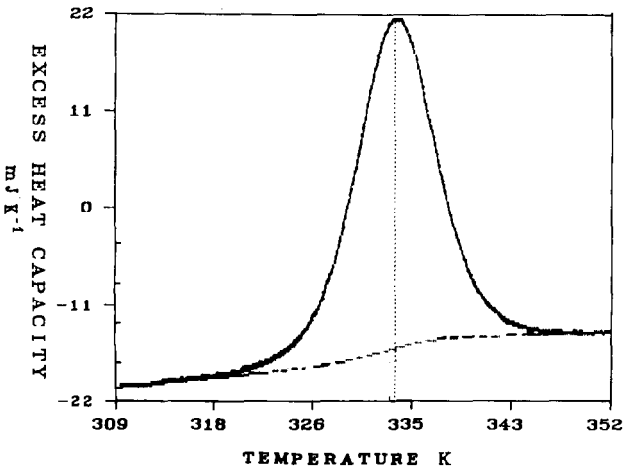

Fig. 3. DSC thermal scan number 53 (2.23 mass% ribonuclease A in 0.2 M glycine buffer at 3.78 pH) scan rate = 18 K h^{-1}. Two-state model curve (· · · · · ·). Only the two-state model baseline under the transition curve is distinguishable.

Repeated thermal scans of a sample exhibited similar transition profiles with the appearance of a slight shoulder near the onset of the transition and an overall decrease in the excess heat capacity. The magnitude of this decrease depended on the conditions of the thermal scan. For example, a repeated scan from 298 to 363 K of a transition at 311.5 K showed a 65% decrease in the value of N which was determined, but no change in ΔH. In contrast, a repeated scan over the same temperature range of a transition at 334.8 K showed only a 39% decrease in the value of N. This behavior suggests an irreversible sample degradation at high temperatures, with the extent of the degradation depending on the maximum temperature of the scan, the scan rate, and the pH. This is consistent with the studies of Zale and Klibanov [16] who showed that ribonuclease A undergoes irreversible hydrolysis of the peptide bonds at the aspartic acid residues and deamination of asparagine and/or glutamine residues at 363 K and pH 4. That ΔH_m remains unchanged shows that the product(s) of the thermal degradation do not interfere with the thermal analysis of the ribonuclease A denaturation. However, only the results for the first scan are reported for the samples studied.

Thermodynamic information on the denaturation transition of ribonuclease A from all sources, determined from DSC thermal scans of 69 dialyzed samples, is summarized in Table 2. Included in Table 2 are results from two samples run at a scan rate of 5 K h^{-1} (scans no. 45 and 46) and two samples at 60 K h^{-1} (scans no. 47 and 48) for comparison with the results determined at the usual scan rate of 18 K h^{-1}. The number of moles undergoing the two-state transition, the transition temperature, the change in the heat capacity of the solution, and the calculated transition enthalpy

ΔH_m were determined by a least-squares fit of the heat capacity data to the two-state model as described above. In addition, several alternative methods were used to evaluate the transition enthalpy and these are also compared in Table 2. The value of ΔH_s was calculated from the area above the sigmoidal baseline generated by the fit to the two-state model divided by the number of moles of material as determined by the spectroscopic analysis. The value of ΔH_l was calculated from the area above a straight line drawn between the estimated ends of the transition divided by the number of moles of material as determined by the spectroscopic analysis. The value of ΔH_v was calculated from a traditional van't Hoff analysis summarized briefly as follows. The extent of reaction $\theta(T)$ is defined as the fractional area up to a temperature T compared with the total area under the transition profile. The equilibrium constant $K(T)$ is related to $\theta(T)$ through $K(T) = \theta(T)/(1 - \theta(T))$. From the equilibrium constant, $K(T)$, the van't Hoff enthalpy ΔH_v is obtained from the slope of a plot of ln K vs. $1/T$

$$\mathrm{d} \ln K/\mathrm{d}T = -\Delta H_v/RT^2 \tag{13}$$

All four measures of the transition enthalpy and the transition temperature were analyzed as linear functions of pH, and all four measures of the transition enthalpy were analyzed as linear functions of the transition temperature. The scatter in the data from these linear least squares fits was considerably larger than the standard deviations of ΔH_m and T_m resulting from the least squares fit of individual profiles to the two-state model. As already noted, systematic patterns could be seen in the residuals $(\mathrm{d}Q/\mathrm{d}T)_{obs} - (\mathrm{d}Q/\mathrm{d}T)_{calc}$ far in excess of the random scatter in the $\mathrm{d}Q/\mathrm{d}T$ measurements. This indicates that room for improvement exists in both the mathematical model and experimental control.

Transition temperature dependence on pH and concentration of ribonuclease A

The transition temperature was found to vary linearly with the pH of the glycine–HCl buffered solution over the range 2–4 and with the concentration of ribonuclease A over the range 1–2.3 mass% according to the equation

$$T_m = 335.1 \pm 0.7 + 11.4 \pm 0.6 \times (\mathrm{pH} - 4) + 2.5 \pm 1.9 \times (\mathrm{mass\%} - 2.0)$$

where the uncertainties represent 99% confidence limits assuming a Student's t distribution for the estimated errors.

Since the glycine–HCl buffer is most effective as a buffer in the pH range 2–4, most of the measurements were performed in this range. The increase of transition temperature with pH in the acidic region has been observed for other globular proteins [6]. This increase has been explained as a stabilization of the native protein brought about by a decrease in its net positive charge as the solution becomes less acidic [3]. Above pH 4, the dependence of T_m on pH levels off. This leveling off has also been reported elsewhere [6],

TABLE 2

Thermodynamic properties of the ribonuclease A transition in solution

Scan no.	Sample		pH	Amount [b] (μmol)	N [c] (μmol)	C_p [c] (kJ mol^{-1} K^{-1})	T_m [c] (K)	ΔH_m [c]	ΔH_s [d]	ΔH_v [e]	ΔH_l [f]
	ID [a]	Mass%									
1[†]	*d*r2	1.93	2.43	1.512	1.325	6.35	310.7	3.11	2.68	3.27	2.95
2	*a*r2	2.00	1.86	0.683	0.587	2.14	311.3	3.14	2.66	3.33	2.96
3	*c*f2	2.01	1.95	0.718	0.628	1.18	311.5	3.10	2.70	3.11	3.23
4	*c*f1	1.73	2.00	0.637	0.555	2.91	311.5	3.11	2.66	3.26	2.97
5	*c*r1	1.73	2.00	0.637	0.569	1.29	311.8	3.08	2.71	3.19	3.01
6	*c*f1	1.14	2.01	0.420	0.371	2.77	311.8	3.11	2.70	3.24	3.14
7	*c*r1	1.83	2.19	0.673	0.554	3.47	313.4	3.12	2.88	3.18	3.22
8	*a*f2	1.85	2.24	0.680	0.613	4.51	313.5	3.20	2.86	3.16	3.08
9	*a*r2	1.85	2.24	0.680	0.612	3.80	313.6	3.22	2.86	3.31	3.08
10	*c*f2	2.08	2.08	0.763	0.727	0.72	315.1	3.23	3.03	3.33	2.95
11	*c*r2	2.08	2.08	0.763	0.666	1.16	315.1	3.31	2.82	3.58	3.11
12	*a*f2	1.63	2.43	0.850	0.786	1.55	315.8	3.14	2.85	3.33	3.30
13	*a*r2	1.63	2.43	0.838	0.781	4.51	315.5	3.11	2.82	3.33	3.33
14	*c*f2	2.07	2.44	0.763	0.723	1.15	315.8	3.28	3.04	3.47	3.42
15[†]	*b*f2	2.00	2.80	0.974	0.951	4.45	316.8	3.17	3.07	3.24	3.14
16[†]	*b*r2	2.00	2.80	0.974	0.890	0.10	317.4	3.27	2.89	3.51	3.17
17	*a*f2	1.93	2.59	0.728	0.768	5.22	317.6	3.28	3.41	3.36	3.51
18	*a*r2	1.93	2.59	0.728	0.725	4.52	317.7	3.35	3.28	3.48	3.31
19	*c*f1	1.85	2.60	0.679	0.655	2.63	318.8	3.35	3.18	3.48	3.26
20	*c*r1	1.85	2.60	0.679	0.591	8.39	318.3	3.40	2.88	3.58	3.45
21	*c*f2	2.08	2.62	0.767	0.810	2.92	319.9	3.31	3.45	3.42	3.54
22	*c*r2	2.08	2.62	0.767	0.718	4.50	319.8	3.42	3.13	3.57	3.35
23	*c*f2	2.07	2.77	0.762	0.747	3.13	320.5	3.52	3.39	3.69	3.65
24	*c*r2	2.07	2.77	0.762	0.756	1.42	320.7	3.54	3.43	3.74	3.57
25	*a*f2	2.06	2.98	0.757	0.784	3.56	322.6	3.54	3.61	3.65	3.58
26	*a*r2	2.06	2.98	0.757	0.808	5.32	322.5	3.50	3.68	3.56	3.63
27	*c*f1	1.85	3.00	0.682	0.665	6.27	323.8	3.56	3.38	3.67	3.25

28	*c*r1	1.85	3.00	0.682	0.633	9.00	323.7	3.55	3.19	3.76	3.61
29	*c*f2	2.09	3.05	0.768	0.831	3.34	324.3	3.61	3.85	3.64	3.87
30	*c*r2	2.09	3.05	0.768	0.807	1.62	324.5	3.68	3.80	3.92	3.71
31	*c*f2	2.06	3.00	0.759	0.791	3.30	324.5	3.48	3.51	3.66	3.82
32	*c*r2	2.06	3.00	0.759	0.736	4.36	324.4	3.56	3.37	3.74	3.77
33†	*b*f2	2.06	3.63	1.05	1.03	3.10	325.5	3.50	3.41	3.51	3.60
34†	*b*r2	2.06	3.63	1.05	0.993	2.55	325.6	3.51	3.31	3.50	3.78
35†	*d*f2	1.04	3.45	0.293	0.294	4.19	325.4	3.46	3.43	3.48	3.77
36†	*d*r2	1.04	3.45	0.290	0.321	8.72	324.8	3.33	3.60	3.38	3.11
37	*a*f2	2.07	3.21	0.760	0.793	3.00	326.7	3.69	3.80	3.75	3.79
38	*a*r2	2.07	3.21	0.760	0.804	6.08	326.5	3.66	3.83	3.64	3.73
39	*b*f2	2.13	3.15	1.11	1.12	3.04	327.5	3.75	3.76	3.71	4.03
40	*b*r2	2.13	3.15	1.11	1.06	2.42	327.6	3.81	3.59	3.86	4.03
41	*c*f1	1.89	3.44	0.694	0.732	4.26	327.6	3.62	3.76	3.69	4.21
42	*c*r1	1.89	3.44	0.694	0.738	3.11	329.8	3.73	3.91	3.63	4.19
43	*a*f2	1.95	3.51	0.716	0.795	4.93	330.1	3.77	4.17	3.60	4.13
44	*a*r2	1.95	3.51	0.716	0.745	5.31	330.2	3.88	3.98	3.97	3.94
45†	*a*f2s	1.95	3.87	0.880	0.973	5.61	331.7	3.75	4.05	3.76	3.71
46	*a*r2s	1.95	3.87	0.880	0.999	2.46	332.0	3.75	4.19	3.82	4.17
47†	*a*f2f	1.95	3.87	0.880	0.879	2.72	334.7	3.85	3.83	4.02	3.94
48†	*a*r2f	1.95	3.87	0.880	0.858	3.64	334.5	3.89	3.77	4.08	3.89
49	*c*f2	2.26	3.55	0.833	0.876	3.40	331.2	3.90	4.08	3.75	4.30
50	*c*r2	2.26	3.55	0.833	0.918	3.07	331.2	3.85	4.23	3.58	4.12
51	*a*f2	1.69	3.87	0.881	0.957	0.91	332.8	3.77	4.04	3.87	4.25
52	*a*r2	1.69	3.87	0.881	0.996	3.07	332.6	3.71	4.15	3.75	4.36
53	*a*f2	2.23	3.78	0.819	0.798	3.08	333.5	4.15	4.02	4.16	4.13
54	*a*r2	2.23	3.78	0.819	0.849	5.69	333.3	4.04	4.19	3.93	4.23
55	*c*f2	2.23	3.94	0.822	0.867	2.35	334.2	4.15	4.41	3.78	4.51
56	*b*f2	1.94	3.93	1.01	1.03	2.86	334.7	4.27	4.33	4.23	4.55
57	*b*r2	1.94	3.93	1.01	0.969	2.55	334.7	4.37	4.13	4.44	4.56
58	*c*f2	2.22	3.99	0.818	0.872	3.82	334.6	4.22	4.47	4.07	4.47
59	*c*r2	2.22	3.99	0.818	0.871	1.88	334.8	4.22	4.48	4.12	4.51
60†	*c*f1	2.03	4.00	0.748	0.748	5.04	334.8	4.29	4.27	4.19	4.46

(continued)

TABLE 2 (continued)

Scan no.	Sample ID [a]	Mass%	pH	Amount [b] (μmol)	N [c] (μmol)	C_p [c] (kJ mol^{-1} K^{-1})	T_m [c] (K)	ΔH_m [c]	ΔH_s [d]	ΔH_v [e]	ΔH_l [f]
61†	*c*r1	2.03	4.00	0.748	0.767	0.97	335.1	4.23	4.29	4.29	4.46
62†	*a*f2	2.09	4.08	0.768	0.791	3.23	335.4	4.37	4.48	4.27	4.44
63†	*a*r2	2.09	4.08	0.768	0.801	4.54	335.3	4.34	4.51	4.17	4.52
64†	*a*f2	2.15	4.53	0.790	0.755	1.34	335.7	4.48	4.30	4.17	4.28
65†	*a*r2	2.15	4.53	0.790	0.730	2.82	335.7	4.56	4.18	4.48	4.12
66†	*c*f2	2.12	4.20	0.781	0.763	3.24	335.7	4.48	4.32	4.31	4.49
67†	*c*r2	2.12	4.20	0.781	0.744	8.09	335.6	4.47	4.15	4.38	4.72
68†	*c*f2	2.05	5.00	0.755	0.646	4.08	335.8	4.83	4.13	4.83	4.47
69†	*c*r2	2.05	5.00	0.756	0.692	4.81	335.8	4.74	4.29	4.55	4.44

[a] The sample is described by three characters consisting of the following: *a*, *b*, *c*, or *d* for the first character which describes the commercial source of the ribonuclease A; f or r for the second character which denotes which of the two sample cells was used; and 1 or 2 for the last character which denotes whether the glycine buffer was 0.2 M (2) or 0.1 M (1). The commercial sources were as follows: *a* for the 90% purity sample; *b* for the 70% purity sample which had been stored in the freezer for 7 years; *c* for the 87% purity sample from the second supplier; and *d* for the 98% purity sample from the third supplier. All the scans except for 45, 46, 47, and 48 were performed at a scan rate of 18 K h^{-1}. Scans 45 and 46, denoted by the letter s added on to the end of the sample description, were performed at 5 K h^{-1} and scans 47 and 48, denoted by the letter f, were performed at 60 K h^{-1}. Scans excluded from the analyses of ΔH as a function of pH or T_m are marked with † (see text for details).

[b] Amount added to cell as determined by spectroscopy and enzymatic activity.

[c] From least-squares fit to a two-state model. Values of ΔH in 100 KJ mol^{-1}.

[d] From area above sigmoidal baseline divided by the amount added. Values of ΔH in 100 kJ mol^{-1}.

[e] From a van't Hoff plot of ln K vs. $1/T$. Values of ΔH in 100 kJ mol^{-1}.

[f] From the area above

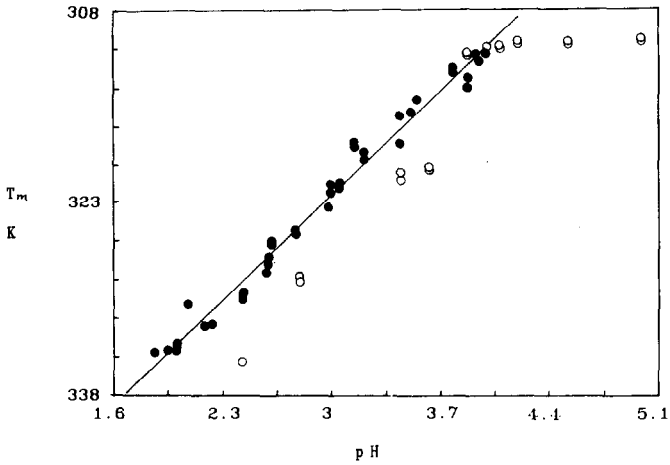

Fig. 4. Plot of the transition temperature dependence on pH in a glycine–HCl buffered solution. The line is the least-squares fit of T_m to pH, $T_m = 333.3 + 11.8(\text{pH} - 3.81)$ and the circles are the points deleted from the fit.

though at a somewhat higher pH and lower concentration of ribonuclease A. The leveling off may be a result of a lack of effectiveness of the glycine–HCl buffer, possible conformational changes in the ribonuclease A, or a combination of both. As a result, all of the analyses summarized in this study include only those data for pH less than 4.

Preliminary DSC measurements of the ribonuclease A transition in 0.2 M sodium acetate–acetic acid buffered solutions exhibited a similar increase of transition temperature with pH but shifted approximately 1.0 pH unit higher than those observed with the glycine buffer. For example, a transition temperature of 334.8 K is observed at pH 4.0 in the glycine buffer, but at pH 5.0 in the sodium acetate buffer. Ginsburg and Carroll [17] have shown that the transition temperature of ribonuclease A at pH 2.1 depends on the buffer, and will increase by as much as 15 K when the buffer is changed from a potassium chloride–hydrochloric acid buffer to a sodium sulfate–sulfuric acid buffer.

The dependence of the transition temperature on pH shown in Fig. 4 is, thus, unique to the glycine–HCl buffer. The glycine buffer was used since the enthalpy of ionization of the buffer is close to that of the amino acid residues of the ribonuclease A. This insures practically complete compensation of the protein ionization heat effects by the buffer ionization heat effects during denaturation so that the measured enthalpy of transition is essentially the enthalpy of the conformational change of the protein [6].

The dependence of the transition temperature on concentration, 2.5 ± 1.9 K per mass% of ribonuclease A, is less well determined but nevertheless statistically significant. Additional measurements over a much wider range of concentration could improve the reliability of this number, but at higher

concentrations, interactions between ribonuclease A molecules are expected to contribute to the energetics and reversibility of the denaturation.

Transition enthalpy dependence on temperature and pH

The various enthalpy values ΔH_m, ΔH_s, ΔH_l, and ΔH_v listed in Table 2 in the range pH 2–4 were fitted by least-squares to a linear dependence on $(T - T_0)$ and $(\mathrm{pH} - \mathrm{pH}_0)$ where the reference temperature was taken to be 333.15 K (60 °C) and the reference pH 3.81. The reference temperature of 333.15 K (60 °C) was adopted rather than the conventional 298.15 K (25 °C) because the latter falls outside the range of all of the measurements in this study. The reference pH is that for which a plot of T_m vs. pH gives the reference temperature 333.15. Choosing the reference pH in this way allows a more explicit comparison of the temperature and pH dependence of the transition enthalpy. The results of these analyses are given in Table 3. Outliers were identified and excluded from these and subsequent analyses. An outlier was defined as a DSC profile for which the measured values of at least three of the five parameters T_m, ΔH_m, ΔH_s, ΔH_l, and ΔH_v differed by more than two standard deviations from their values calculated from a fit of the parameters to a linear function of pH. Outliers are identified in Table 2 as are those data for which the pH was $\geqslant 4$. It should be noted that three of the four measurements that were made at slow and fast scan rates were among those identified as outliers.

The standard deviations of the linear fits ranged from 10.7 (ΔH_m vs. T_m) to 15.1 kJ M^{-1} (ΔH_v vs. T_m) which correspond respectively to errors on the order of 2.7% to 3.8% in individual enthalpy determinations. In the graphs of ΔH_m (Fig. 5) and ΔH_v (Fig. 7), a pronounced upswing in the measured data is noted above approximately 334 K corresponding to pH 3.9. This

TABLE 3

Transition enthalpies of ribonuclease A in solution as a function of transition temperature and pH

Transition enthalpy	Result of linear fit to T_m $\Delta H = \Delta H_0 + \Delta H' (T_m - T_0)$ [a]			Result of linear fit to pH $\Delta H = \Delta H_0 + \Delta H'' (\mathrm{pH} - \mathrm{pH}_0)$ [a]		
	ΔH_0 (kJ mol^{-1})	$\Delta H'$ (kJ K^{-1} mol^{-1})	σ(fit) (kJ mol^{-1})	ΔH_0 (kJ mol^{-1})	$\Delta H''$ (kJ pH^{-1} mol^{-1})	σ(fit) (kJ mol^{-1})
ΔH_m	399.9 ± 2.5	4.3 ± 0.2	10.7	399.4 ± 2.9	50.4 ± 2.7	12.4
ΔH_s	421.1 ± 3.4	7.0 ± 0.3	14.7	421.3 ± 3.5	82.8 ± 3.3	15.1
ΔH_v	396.0 ± 3.3	3.3 ± 0.3	14.3	395.6 ± 3.5	38.6 ± 3.3	15.1
ΔH_l	430.9 ± 3.2	6.1 ± 0.3	13.8	431.3 ± 3.1	72.09 ± 3.0	13.5

[a] The reference conditions are $T_0 = 333.15$ K (60 °C) and $\mathrm{pH}_0 = 3.81$, the pH at which a plot of T_m vs. pH gave the reference temperature T_0.

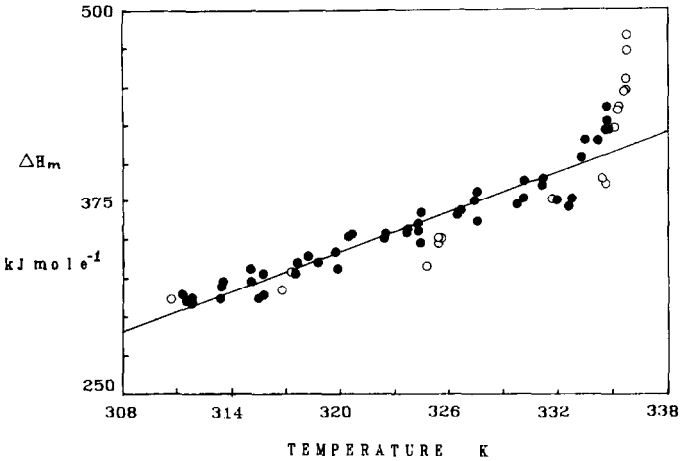

Fig. 5. Plot of the values of ΔH_m as a function of transition temperature. The line is the least-squares fit of ΔH_m to T_m, $\Delta H_m = 339.9 + 4.3(T_m - 333.15)$ and the circles are the points deleted from the fit.

upswing corresponds to the leveling off of the dependence of T_m on pH noted above. The dependence of ΔH_m and ΔH_v on pH show no leveling off above pH 4 in Table 2, although the dependence of ΔH_s (Fig. 6) and ΔH_l on pH do. ΔH_m and ΔH_v are determined from the shape of the temperature profiles as functions of temperature and represent different methods for calculating the van't Hoff enthalpy. Values of ΔH_s and ΔH_l are calculated from the area of the transition profile divided by the number of moles of

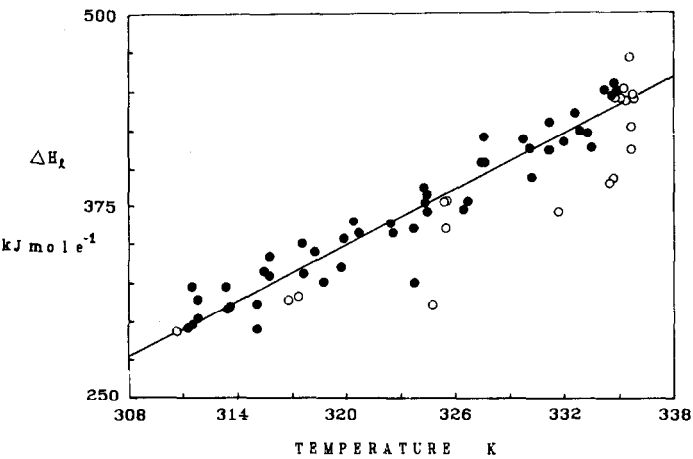

Fig. 6. Plot of the values of ΔH_l as a function of transition temperature. The line is the least-squares fit of ΔH_l to T_m, $\Delta H_l = 430.9 + 6.1(T_m - 333.15)$ and the circles are the points deleted from the fit.

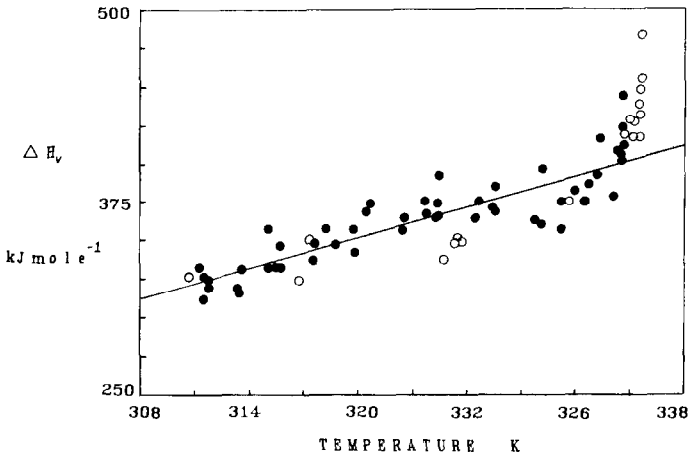

Fig. 7. Plot of the values of ΔH_v as a function of transition temperature. The line is the least-squares fit of ΔH_v to T_m, $\Delta H_v = 396.0 - 3.3(T_m - 333.15)$ and the circles are the points deleted from the fit.

material known to be present in the cell. We therefore expect the dependence of ΔH_m and ΔH_v on pH to be similar and the dependence of ΔH_s and ΔH_l on pH to be similar. In addition to the difference in behavior between ΔH_m (or ΔH_v) and ΔH_s (or ΔH_l) at high pH, comparison of their linear dependencies on transition temperature reported in Table 3 also shows a pronounced difference both in slope and in their values at the reference temperature of 333.15 K. This difference defines the degree of cooperativity of the transition as will be discussed below.

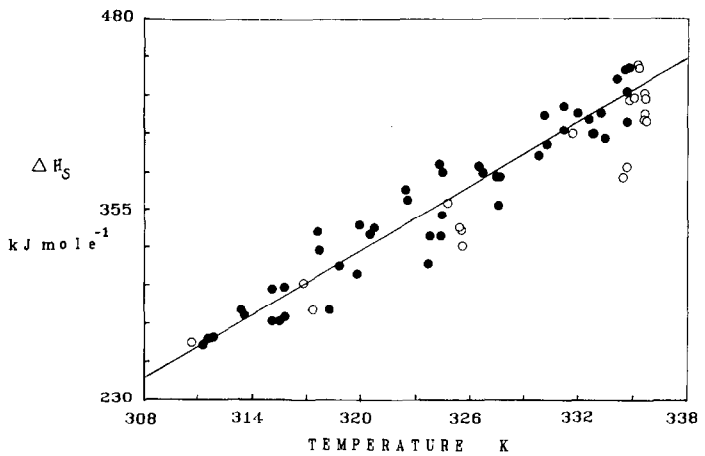

Fig. 8. Plot of the values of ΔH_s as a function of transition temperature. The line is the least-squares fit of ΔH_s, $\Delta H_s = 421.1 + 7.0(T_m - 333.15)$ and the circles are the points deleted from the fit.

The comparison of the least-squares fits reported in Table 3 also shows that the fits of ΔH vs. T_m are equivalent to ΔH vs. pH (after the so-called outliers have been removed), both in the standard deviations of the fits, the values of ΔH_0 and the correspondence of the ratio of the slopes to the slope of T_m vs. pH. Plots of the various enthalpy values versus transition temperature are shown in Figs. 5–8.

Simulated profile shapes were calculated in which (i) a fraction of the protein was assumed to be associated as dimers in the low temperature globular state but fully dissociated following denaturation; (ii) a fraction of the protein was assumed to decompose into two fragments through breakage of peptide bonds following denaturation; and (iii) a fraction of the denatured protein was assumed to be associated as dimers. Either of the latter two effects could account for the loss of repeatability of the temperature profiles described in this and earlier studies [3,6]. These simulated profiles were then analyzed in the same manner as the ribonuclease A data. In all three cases, the transition temperature was unaffected within measurement error. For the two cases of association, either pre- or post-transition, ΔH_m increased and N decreased by about 3.5% for 20% association while the profile area remained unaffected. The degree of change in ΔH_m and N will depend upon the extent of association. For the case of decomposition ΔH_m decreased and N increased by about 6% for 20% decomposition while the profile area decreased by about 1%. The degree of change in ΔH_m and N will depend upon the number of fragments formed by the decomposition. Because the profile area is relatively insensitive to the effects of association or dissociation, the values of ΔH_s and ΔH_l will be insensitive as well.

If decomposition through irreversible hydrolysis of the peptide bonds at high pH and T_m as reported by Zale and Klibanov [16] were a predominant effect under the experimental conditions of this study, we would expect to see at higher pH a leveling off of ΔH_m (or ΔH_v), no change in ΔH_s (or ΔH_l) and T_m, and an increase in the apparent cooperativity, N/N_t (discussed below) of the transition. These are exactly opposite to the effects we have observed leading us to conclude that decomposition alone, of the sort reported by Zale and Klibanov [16], is not a problem under the experimental conditions described here.

If pre- or post-transition association were a predominant effect under the experimental conditions of this study, then we would expect to see an increase in the value of ΔH_m (or ΔH_v) with increasing concentration. When ΔH_m is simultaneously fitted to a linear function of T_m and concentration, a slight dependence is noted that is significant at the 95% confidence level but not at the 99% confidence level, where $d\Delta H_m/dC = 19 \pm 22$ kJ mol^{-1} mass%$^{-1}$. Though of marginal significance, the positive sign of $d\Delta H_m/dC$ is consistent with the expected change in ΔH_m.

The irreversibility of the conformational change was more pronounced at high pH and T_m than at low pH and T_m, supporting the notion, in the

absence of dissociation, that association, if it existed, would arise from post-transition association (which would be irreversible) rather than pre-transition association. However, the cooperativity [$\Delta H_s/\Delta H_m = N/N_t$ (see below)] provides a stronger indication that association is greater at low pH so that the irreversibility must arise from other sources, perhaps the existence of denatured conformations with high barriers precluding reformation of the native state.

Temperature dependence of the transition heat capacity change

In addition to the determination of the number of moles participating in the two-state transition, the model also determines the change in the excess molar heat capacity. This change is the difference $\Delta B_0 = N\Delta C_p$ between the linear extrapolations of the pre-transitional baseline and the post-transitional baseline to the transition temperature T_m. For all the scans, the average of this change was 3.6 ± 1.9 kJ K^{-1} mol^{-1} (Table 2). This average is in agreement with the value of 5.2 kJ K^{-1} mol^{-1} obtained by Privalov and Khechinashvili for 0.5 mass% ribonuclease A solutions [6]. The change in excess heat capacity showed no dependence on the transition temperature within the accuracy of the measurements. This was also observed by Privalov and Khechinashvili [6].

The dependence of ΔH on transition temperature can be described by a linear dependence. If the linear increase in ΔH with temperature results from the difference in the heat capacities before and after the denaturation transition, then the derivative $d\Delta H/dT_m$ should be equal to the average value of the change in the heat capacity of the transitional baselines. The values of the slopes of ΔH vs. T_m for all four measures of ΔH_m are given in Table 3. Of particular interest are $d\Delta H_m/dT_m = 4.3 \pm 0.2$ kJ K^{-1} mol^{-1} and $d\Delta H_s/dT_m = 7.0 \pm 0.3$ kJ K^{-1} mol^{-1}. The former is more consistent with the value obtained from the shift in baseline.

Cooperativity of the transition

Implicit in the least-squares fit to the two-state model is the notion that the transition is fully cooperative, i.e. the number of moles of A plus the number of moles of B is equal to N, the number of moles of material undergoing the transition. There is, however, some question as to whether the ribonuclease A transition fully conforms to a two-state transition. Privalov [18] showed that the unfolding transition for a number of globular proteins, including ribonuclease A, was not purely two state since the ratio of the experimental transition enthalpy to the van't Hoff enthalpy was consistently 1.05 ± 0.03. He defined an effective enthalpy ΔH_{eff} as

$$\Delta H_{eff} = 4RT_m^2 h_m/\text{area} \tag{14}$$

where h_m is the peak height at T_m and T_m is the temperature corresponding to half the area of the transition profile above the baseline. The cooperativity C was then defined as

$$C = \Delta H/\Delta H_{eff} \tag{15}$$

where ΔH is the area under the transition profile divided by number of moles added to the calorimeter cell N_t. Equation (14) follows directly from eqn. (9) by substituting $K = 1$, the value of K at half the area and recognizing that $N\Delta H$ is the area under the peak above the baseline. An alternate method for defining the cooperativity, however, is the ratio of N, the value obtained from the least-squares fit of the two-state model, to the value of N_t determined spectroscopically, i.e. $C = N/N_t$. Alternately, but equivalently, we can use our definitions of $\Delta H_m = \text{area}/N$ and $\Delta H_s = \text{area}/N_t$ to define C as $\Delta H_s/\Delta H_m$.

Values of $\Delta H_s/\Delta H_{eff}$ and N/N_t are compared in Table 4 as a function of the transition temperature T_m. Both measures of C showed a discernible trend as a function of T_m over the pH range 2–4, and a least-squares fit of C to $T_m - 333.15$ gave

$$C = \Delta H_s/\Delta H_{eff} = 1.075 \pm 0.017 + (0.009 \pm 0.001)(T_m - 333.15)$$

$$C = N/N_t = 1.057 \pm 0.014 + (0.007 \pm 0.001)(T_m - 333.15)$$

$$C = \Delta H_s/\Delta H_m = 1.059 \pm 0.012 + (0.008 \pm 0.001)(T_m - 333.15)$$

Since substitution of eqns. (9)–(12) at $T = T_m$ into eqns. (14) and (15) results in $\Delta H_s/\Delta H_{eff} = N/N_t$, it was expected that these two measures of the cooperativity should agree and show a comparable dependence on T_m. When data above pH 4 were included, the cooperativity showed a downward trend corresponding to the leveling off of T_m as a function of pH.

Privalov and Khechinashvili examined the cooperativity of five globular proteins as a function of T_m and found a random scatter about a constant value of 1.05 ± 0.03 [6]. Close inspection of the ribonuclease A data appearing in their fig. 8 showed a similar increase in C up to $T_m = 60\,^\circ\text{C}$ with a downward trend above 60 °C. However, the number of data points appearing in their figure was insufficient to make a quantitative determination of the slope.

The change in cooperativity as a function of pH and, consequently T_m, is a direct consequence of the breakdown in the two-state model as suggested by Privalov and Khechinashvili [6]. The most likely source of the deviation of the cooperativity from unit is the existence of intermediate or metastable states in the denaturation, the nature of which would be expected to be functions of pH and other environmental variables. Nevertheless, that the data span the ideal value of 1.0 suggests that: (i) the two-state model does afford a reasonable basis for the systematic determination of transition enthalpies and heat capacities for this system; (ii) the value of N obtained

TABLE 4

The cooperativity of the ribonuclease A transition in solution

Scan no.	Transition temperature (K)	Cooperativity		Scan no.	Transition temperature (K)	Cooperativity	
		$N/$ Amount [a]	$\Delta H_s/\Delta H_{eff}$ [b]			$N/$ Amount [a]	$\Delta H_s/\Delta H_{eff}$ [b]
1 †	310.7	0.876	0.841	36	324.8	1.11	1.02
2	311.3	0.859	0.823	37	326.7	1.04	0.990
3	311.5	0.875	0.852	38	326.5	1.06	1.06
4	311.5	0.870	0.856	39	327.5	1.01	1.19
5	311.8	0.893	0.861	40	327.6	0.953	1.10
6	311.8	0.883	0.859	41	327.6	1.05	1.04
7	313.4	0.939	0.865	42	329.8	1.06	1.08
8	313.5	0.903	0.850	43	330.1	1.11	1.12
9	313.6	0.901	0.870	44	330.2	1.04	1.02
10	315.1	0.953	1.06	45 †	331.7	1.11	1.04
11	315.1	0.873	0.819	46	332.0	1.14	1.06
12	315.8	0.925	0.874	47 †	334.7	1.00	1.00
13	315.5	0.932	0.870	48 †	334.5	0.975	0.955
14	315.8	0.948	0.920	49	331.2	1.05	1.020
15 †	316.8	0.912	0.956	50	331.2	0.907	1.103
16 †	317.4	0.853	0.852	51	332.8	1.09	1.082
17	317.6	1.08	1.020	52	332.6	1.13	1.124
18	317.7	1.02	0.980	53	333.5	0.974	0.980
19	318.8	0.799	0.966	54	333.3	1.04	1.04
20	318.3	0.963	0.823	55	334.2	1.06	1.10
21	319.9	0.870	1.040	56	334.7	1.02	1.02
22	319.8	1.04	1.145	57	334.7	0.958	0.939
23	320.5	0.936	0.949	58	334.6	1.07	1.08
24	320.7	0.980	0.962	59	334.8	1.07	1.06
25	322.6	0.992	0.988	60 †	334.8	1.00	1.00
26	322.5	1.04	1.06	61 †	335.1	1.03	0.982
27	323.8	0.974	0.901	62 †	335.4	1.03	1.04
28	323.7	0.927	0.880	63 †	335.3	1.04	1.06
29	324.3	1.08	1.10	64 †	335.7	0.870	1.02
30	324.5	1.05	1.04	65 †	335.7	0.924	0.922
31	324.5	1.04	0.988	66 †	335.7	0.977	0.976
32	324.4	0.970	0.939	67 †	335.6	0.952	0.941
33 †	325.5	0.958	0.962	68†	335.7	0.856	0.903
34 †	325.6	0.924	0.789	69†	335.8	0.916	0.887
35 †	325.4	1.00	1.00				

[a] $N/N_t = 1.057 \pm 0.014 + (0.007 \pm 0.001)(T_m - 333.15)$.

[b] $\Delta H_s/\Delta H_{eff} = 1.075 \pm 0.017 + (0.009 \pm 0.001)(T_m - 333.15)$.

† Scans excluded from the analyses of ΔH as a function of pH or T_m.

from two-state analysis is a reasonable estimate for the number of moles of material participating in the transition; and (iii) the temperature at which the cooperativity = 1.0 would be a suitable choice for defining the melting temperature.

Analysis of errors in the enthalpy data

A purpose of reference data is to allow individuals to assess the accuracy of their own measurements and to draw conclusions from comparisons of data from different substances or from the same substance under varying conditions. In the preceding sections we have examined the effects of pH, choice of buffer, and concentration of ribonuclease A on the transition temperature, enthalpy, and heat capacity change. Additional factors include experimental variability and data-analysis methods.

The effects of source of ribonuclease A and buffer concentration were assessed by comparing the results of analyses of subsets of the ribonuclease A data. As a basis for the comparison, a linear least-squares fit of ΔH_m to $T_m - 333.15$ for each subset of data was performed. These data are reported in Table 5.

Concerning the dependence of ΔH_m on sample origin, samples *a* and *c* agreed with each other and with the analysis of the combined data. Sample *b*, the sample of least purity (70%) that had been stored in a freezer for seven years, appeared to deviate slightly from the overall average of the data, but with only two degrees of freedom, this difference is somewhat speculative. An insufficient number of measurements were made with sample *d* to draw any conclusions. It appears that the measured molar enthalpy of transition, ΔH_m, is not very sensitive to the source of the material.

A comparison of the data from the 0.1 M buffer solution with the data from the 0.2 M buffer solution did appear to show a significant difference

TABLE 5

Measured transition enthalpies of ribonuclease A in solution as a function of experimental conditions. Results of the linear fit $\Delta H_m = \Delta H_{m0} + \Delta C_{p0}(T - T_0)$, $T_0 = 333.15$ K (60 °C)

Data set [a]	ΔH_{m0} (kJ mol^{-1})	ΔC_{p0} (kJ mol^{-1} K^{-1})	σ(fit) (kJ mol^{-1})	ν
All data	399.9 ± 5.0 [b]	4.34 ± 0.40	10.7	47
Front cell, all sources	400.9 ± 6.8	4.47 ± 0.54	10.0	23
Right cell, all sources	398.8 ± 8.1	4.21 ± 0.66	11.8	22
Sample *a*	391.1 ± 8.3	3.85 ± 0.68	10.5	16
Sample *b*	420.3 ± 13.8	7.56 ± 3.40	5.7	2
Sample *c*	400.5 ± 6.0	4.34 ± 0.45	8.2	25
0.1 M buffer solution	386.1 ± 6.2	3.53 ± 0.39	3.6	8
0.2 M buffer solution	401.3 ± 5.7	4.44 ± 0.51	11.5	37

[a] Sample *a*: 90% purity; sample *b*: 70% purity, stored for 7 hears; sample *c*: 87% purity ribonuclease A. Only those data between pH 2 and 4 not identified as outliers in Table 2 were used in the analysis.

[b] All uncertainties represent 95% confidence limits based on the standard deviation of the fit σ, the number of degrees of freedom ν (= no. of observations − 2), and a Student's *t* distribution.

between the two as can be seen in Table 5. However, when the combined data were fitted simultaneously to a linear function in T_m and buffer concentration, the coefficient of the buffer concentration term could not be distinguished from zero. Therefore, we conclude that for the range of buffer concentrations used in this study, no dependence of ΔH_m on buffer concentration could be discerned.

The comparison of analyses of data from the right/left pair of cells in the calorimeter to those from the front/back pair of cells has provided some insight into the origin of the scatter in the calorimetric data. The data in Table 5 indicate no difference in the values of ΔH_{m0} and ΔC_{p0} between the two pairs of cells. However, an analysis of ΔH_m, ΔH_s, and T_m as functions of pH for the right/left pair of cells and for the front/back pair of cells compared to an analysis of the difference in ΔH_m, ΔH_s, and T_m between the front/back and right/left cells shows that the scatter of data in the analysis of differences is less than the scatter for either pair of cells individually. This comparison is presented in Table 6. If the scatter in data were completely random then the standard deviation of the least-squares fit of the difference between the front/back and right/left cells would have been approximately $\sqrt{2}$ times the standard deviation of the fit of the front/back or right/left data. Since the standard deviation of the analysis

TABLE 6

A comparison of analyses of data from the front/back pair of cells and the right/left pair of cells with the difference between the pairs of cells [a]

$T_m = T_{m0} + T'_{m0}$ (pH − 3.81)	T_{m0} (K)	T'_{m0} (K pH^{-1})	σ(fit) (K)
Right/left cells	333.37 ± 0.38	11.86 ± 0.39	1.06
Front/back cells	333.21 ± 0.38	11.76 ± 0.39	1.06
Right/left − back/front	0.24 ± 0.19	0.14 ± 0.19	0.52
$\Delta H_m = \Delta H_{m0} + \Delta H'_{m0}$ (pH − 3.81)	ΔH_{m0} (kJ mol^{-1})	$\Delta H'_{m0}$ (kJ pH^{-1} mol^{-1})	σ(fit) (kJ mol^{-1})
Right/left cells	401.8 ± 4.8	51.7 ± 4.9	13.3
Front/back cells	400.5 ± 4.3	53.3 ± 4.4	12.0
Right/left − back/front	5.5 ± 2.0	6.4 ± 2.1	5.6
$\Delta H_s = \Delta H_{s0} + \Delta H'_{s0}$ (pH − 3.81)	ΔH_{s0} (kJ mol^{-1})	$\Delta H'_{s0}$ (kJ pH^{-1} mol^{-1})	σ(fit) (kJ mol^{-1})
Right/left cells	421.7 ± 6.0	86.9 ± 6.2	16.7
Front/back cells	421.1 ± 5.7	79.1 ± 5.8	15.7
Right/left − back/front	−0.3 ± 5.2	−7.6 ± 5.4	14.6

[a] Only those experiments where both the right/left and front/back cells were used are included in these analyses. The difference between right/left and front/back cells were the differences for a single scan. Each data set represents twenty-one measurements, and the uncertainties are one standard deviation.

of the differences was half the standard deviation of either of the cell pairs, we conclude that more than half the error must arise from other than completely random sources. Since the amount of material in the cells, the pH, the concentration of ribonuclease A, and the buffer concentration were closely matched in the two pairs of cells, the only remaining source of scatter in the data is in the analysis of the data. Probable sources of error include: (i) contributions to the profile shape from a non-linear background due to incomplete balancing of the blank and sample cells; and (ii) scatter arising from variations in the selection of regions for calculation of baselines and the transition profile. The combination of these two factors appears to contribute a random error of approximately 1% in the enthalpy determination (a standard deviation of 3.96 kJ mol^{-1} out of a total enthalpy of 400 kJ mol^{-1}). The remainder of the error (approximately 3%), which shows up in the analyses of the right/left or front/right cells, arises from between-run differences. The most likely source of this error is in the measurement of pH and variations in cell loading (both pairs of cells contained approximately the same amount of material but the between-run variation was about 30%) which would not be expected to contribute to between-cell-pair differences, since both pairs of cells were filled from the same sample source to the same amount. A 1% error would be caused by an error of 0.08 pH units and when the data corresponding to high cell loading were removed from the fit, the

TABLE 7

Comparison of present work with literature values

Temperature (K)	ΔH_m (100 kJ [a] mol^{-1})	Literature ΔH (100 kJ mol^{-1})	Difference [b]	Ratio ΔH(lit)/ΔH_m	Literature reference
314.2	3.18±0.04	3.52	−0.34	1.107	c
315.6	3.24±0.04	3.35	−0.11	1.034	d
318.1	3.35±0.04	3.72	−0.37	1.110	c
320.1	3.43±0.03	3.97, 3.60	−0.54, −0.17	1.157, 1.050	c,e
323.1	3.56±0.03	3.56	0	1.000	d
326.9	3.73±0.03	4.02	−0.29	1.078	e
327.1	3.74±0.03	4.18	−0.44	1.118	c
329.1	3.83±0.04	3.97, 4.27	−0.14, −0.44	1.037, 1.115	d,c
331.1	3.91±0.04	4.18	−0.27	1.069	d
333.1	4.00±0.05	4.10	−0.10	1.025	d
336.3	4.14±0.06	4.81	−0.67	1.162	c

[a] Calculated from the least squares fit of ΔH_m to T_m. Uncertainties represent two standard deviations in the calculated values.

[b] The average difference is −8.1% relative to the calculated value.

[c] 0.5 Mass%, ref. 6.

[d] 15.0 Mass%, ref. 7.

[e] 2.8 Mass%, ref. 3.

standard deviation dropped from 12.4 to 8.2 kJ mol^{-1}. Cell loading can be expected to affect ΔH_m and T_m because of changes in the cell calibration.

When the analysis of the difference in ΔH_s between front/back and right/left cells is compared with the analysis of ΔH_s for either cell pair, the standard deviations of the analyses are more compatible. This is because the measured value of N_t contributes to the determination of ΔH_s. Scatter in the values of N_t will result from scatter in the cell loading which will be on the order of an additional 1%.

The transition enthalpies obtained in this study are compared in Table 7 with calorimetric determinations of the transition enthalpy reported in the literature. If the literature values are fitted to a linear function of $T - 333.15$ K, the standard deviation of the fit is 19 kJ mol^{-1} and the coefficients and their 95% confidence intervals are $\Delta H_0 = 435 \pm 19$ kJ mol^{-1} and $\Delta C_{p0} = 5.0 \pm 1.8$ kJ mol^{-1} K^{-1}. Since these values were obtained by dividing the area above a linear or stepped baseline by the number of moles of ribonuclease A in the cell, they are most comparable with the values of ΔH_l reported in Table 3 of this study (430.9 ± 3.2 and 6.1 ± 0.3 kJ mol^{-1}, respectively), with which they are in agreement.

CONCLUSIONS

We have demonstrated that the transition temperature and enthalpy of ribonuclease A can be measured with sufficient accuracy and reproducibility to serve as reference data for the evaluation of calorimeter performance. Factors that influence the accuracy of the determination of the transition enthalpy and temperature include cell loading, adequate scan range to allow accurate values for the asymptotic slopes of the baseline to be determined, accuracy of the pH measurements, and non-linear baselines. The transition temperature and enthalpy are both linear functions of pH over the range 2–4 using glycine buffer. Different buffers will give significantly altered values of ΔH and T_m as functions of pH.

We recommend that ΔH_m and ΔH_s values be reported over ΔH_v and ΔH_l values because the latter are not strictly thermodynamically correct and the former are less sensitive to the selection of regions for baseline and profile analyses. The determination of ΔH_v does not include the variation of the transition enthalpy over the temperature range of the transition. A straight baseline as assumed in the determination of ΔH_l is not a realistic representation of the baseline under the transition curve. Use of ΔH_m has the advantage over use of ΔH_s of not requiring knowledge of the amount of material in solution and, under carefully controlled circumstances, the transition profile can be used for quantitative analysis to estimate the molar concentration of protein undergoing the transition. This is a particular advantage when the protein is believed to have been degraded. Use of ΔH_s

has the advantage over use of ΔH_m of not being dependent on a two-state model for its determination. However, both ΔH_m and ΔH_s should be measured and reported because a comparison of the two values yields valuable information on the cooperativity of the transition.

A larger protein would be likely to give a sharper profile than ribonuclease A because of the greater enthalpy per mole, but is more likely to deviate from pure two-state behavior. To be suitable as a reference compound, the material properties should not be too sensitive to sample integrity or history, and it should be possible to model the profile shape in order to evaluate the influence of experimental conditions on observed transition profile. Ribonuclease A satisfies these two criteria.

REFERENCES

1 F.P. Schwarz, Thermochim. Acta, 107 (1986) 37.
2 K. Beck, S.J. Gill, and M. Downing, J. Am. Chem. Soc., 87 (1965) 901.
3 T.Y. Tsong, R.P. Hearn, D.P. Wrathall, and J.M. Sturtevant, Biochemistry, 9 (1970) 2666.
4 P.L. Privalov, N.N. Khechinashvili, and B.P. Atanasov, Biopolymers, 10 (1971) 1865.
5 P.L. Privalov, E.I. Tiktopulo, and N.N. Khechinashvili, Int. J. Peptide Protein Res., 5, (1973) 229.
6 P.L. Privalov and N.N. Khechinashvili, J. Mol. Biol., 86 (1974) 665.
7 I.V. Sochava, T.V. Belopolskaya, and O.I. Smirnova, Biophys. Chem., 22 (1985) 323.
8 F.M. Richards and H.W. Wyckoff, in Paul D. Boyer (Ed.), The Enzymes, Vol. IV, 3rd. edn., Academic Press, New York, 1971, p. 647.
9 M. Kunitz, J. Biol. Chem., 164 (1946) 563.
10 E.M. Crook, A.P. Mathias, and B.R. Rabin, Biochem. J., 74 (1960) 234.
11 L.H. Chang, S.J. Li, T.L. Ricca, and A.G. Marshall, Anal. Chem., 56 (1984) 1502.
12 K. Takahaski and J.M. Sturtevant, Biochemistry, 20 (1981) 6185.
13 K. Weber and M. Osborn, J. Biol. Chem., 224 (1969) 4406.
14 P.D. Ross and R.N. Goldberg, Thermochim. Acta, 10 (1974) 143.
15 E. Calvet and H. Prat, Recent Progress in Microcalorimetry, translated by H.A. Skinner, Macmillan, New York, 1963, p. 385.
16 S.E. Zale and A.M. Klibanov, Biochemistry, 25 (1986) 5432.
17 A. Ginsburg and W.R. Carroll, Biochemistry, 4 (1965) 2159.
18 P.L. Privalov, Adv. Protein Chem., 33 (1979) 167.